

$^{14}\text{N}(p, \gamma)^{15}\text{O}$ reaction measurement at the LNGS Bellotti Ion Beam Facility

A. COMPAGNUCCI⁽¹⁾(²)(*)

⁽¹⁾ *Gran Sasso Science Institute - L'Aquila (AQ), Italy*

⁽²⁾ *INFN, Laboratori Nazionali del Gran Sasso (LNGS) - Assergi (AQ), Italy*

received 31 January 2024

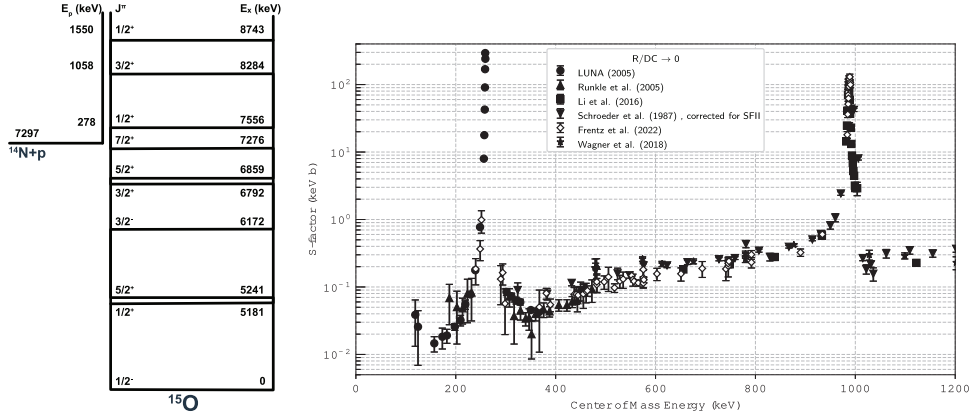
Summary. — $^{14}\text{N}(p, \gamma)^{15}\text{O}$ is an astrophysical key reaction as the bottleneck for the CNO cycle. It directly influences the lifetime of massive stars and solar CNO neutrino flux, a precise extrapolation of its cross-section at astrophysical energies is therefore essential for inferring the solar metallicity. This work reports on the experimental setup and target characterization for a renewed deep-underground measurement of this reaction in the energy range between 0.25 and 1.5 MeV at the 3.5 MV accelerator of the Bellotti Ion Beam Facility. Preliminary cross-section data for the ground-state transition, plus 6.79 MeV and 5.24 MeV secondary transitions are presented.

1. – Introduction

The CNO cycle is the dominant mechanism for energy production in stars slightly more massive than the Sun during the hydrogen burning phase. The $^{14}\text{N}(p, \gamma)^{15}\text{O}$ reaction is the slowest reaction of the CNO cycle and controls its speed and the rate of energy generation of this process. In our Sun $\sim 1\%$ of energy is produced through the CNO cycle, contributing also to 1.6% of the solar neutrino flux [1]. Nevertheless, CNO hydrogen burning in the Sun plays a key role as a tool to infer the chemical composition of the solar core, through the detection of neutrino emission lines from the β^+ decay of ^{13}N and ^{15}O . In fact, solar metallicity is still a matter of debate due to difficulties in reconciling the conflicting results that have been derived from the standard solar model using photospheric abundances and from helioseismic observations [2].

As recently assessed by the Borexino Collaboration, following their recent first direct detection of solar CNO neutrino, $^{14}\text{N}(p, \gamma)^{15}\text{O}$ remains the second major contribution to the uncertainty budget in the estimation of the C and N abundances in the Sun after the CNO neutrino flux itself [3].

(*) On behalf of the LUNA Collaboration.



(a) Level scheme of ^{15}O . (b) Astrophysical S-factor for the ground state transition.

Fig. 1. – On the left, the level scheme of ^{15}O . On the right, the available literature data of the astrophysical S-factor for the ground state transition (refs. [4-9]).

At the energies of astrophysical interests, the total cross-section of $^{14}\text{N}(p,\gamma)^{15}\text{O}$ has its main contributions from the transition to the $E_x = 6.79$ MeV and 6.17 MeV excited states of ^{15}O and to its ground state (fig. 1(b)), which is significantly affected by the high energy tail of a sub-threshold level at $E_r = -505$ keV corresponding to the aforementioned 6.79 MeV excited state (see level scheme in fig. 1(a)).

In our Sun the Gamow peak for the reaction lies between 15 and 50 keV. The $^{14}\text{N}(p,\gamma)^{15}\text{O}$ reaction has been the subject of renewed interest in recent years due to the need for better extrapolations of its cross-section at these energies, not directly accessible by the experiments. In 2011, Adelberger *et al.* [1] conducted a comprehensive evaluation of the reaction cross-section. Including in their *R*-matrix fit the results from Schröder *et al.* [5], LUNA [4, 10], and LENA [6], they concluded that further work was necessary to better constrain the low-energy cross-section. As a result, many new experiments have been carried out, focusing on different aspects of the reaction.

Recent studies by Li *et al.* [7] reported measured differential cross-sections in the energy range $E_p = 0.5$ –3.6 MeV. Their multi-channel *R*-matrix analysis found several inconsistencies between the low-energy data and the extrapolation obtained from higher-energy data, leading to high systematic uncertainty, particularly for the ground-state transition. The work of Wagner *et al.* [9] attempted to bridge the gap with the low-energy data by studying the 6.79 MeV and ground-state transitions in the energy range⁽¹⁾ $E_p = 0.5$ –3.6 MeV. They found significantly higher values for the 6.79 MeV transition (up to 50% above 1 MeV) than those reported by Li *et al.*, reaffirming the inconsistencies.

At the same time, efforts were made to improve the knowledge of parameters needed for a more reliable extrapolation. Daigle *et al.* [11] measured the strength and branching ratios of the $E_p = 278$ keV resonance at LENA, reporting an improved value of the resonance strength $\omega\gamma = 12.6 \pm 0.3$ meV with respect to the previous value recommended by Adelberger *et al.* ($\omega\gamma = 13.1 \pm 0.6$ meV). Frenzt *et al.* [12] measured for the first time

⁽¹⁾ As a general notation, in this work E_p refers to the proton energy in the laboratory reference frame.

the lifetime of the $E_x = 6.79$ MeV sub-threshold state in ^{15}O . However, the uncertainty of this result is still too large to constrain the low-energy R -matrix analysis. An activation measurement was also performed at Atomki by Gyürky *et al.* [13], resulting in a total cross-section data set in the energy range $E_p = 0.6$ – 1.5 MeV potentially hinting at a lack of knowledge in literature data.

More recently a new underground measurement was performed by Frentz *et al.* [8] at the CASPAR accelerator (SURF). Their data, taken between $E_p = 0.28$ – 1.07 MeV tried to close a gap in the existing data sets. In a comprehensive R -matrix analysis of the three most important transitions, they concluded that the main source of uncertainty currently lies in the weaker transitions and in the behavior of the ground-state transition at low energies, specifically calling out for angular distribution measurements below the data set by Li *et al.* [7].

In the following, an experiment project towards a renewed $^{14}\text{N}(\text{p},\gamma)^{15}\text{O}$ underground measurement is reported, the aim of which is to measure the excitation function for the most relevant transitions of the reaction and to have enough sensitivity to probe the weakest ones, over an extended energy range.

2. – Experimental setup

2.1. Accelerator. – The experiment was performed at the 3.5 MV accelerator of the Bellotti Ion Beam Facility (IBF) of the Gran Sasso National Laboratories (LNGS). The newly installed, single-ended electrostatic 3.5 MV accelerator is equipped with an ECR source and is capable of providing an intense proton beam with up to 1 mA of current [14].

During the measurements, a proton beam with $E_p = 0.25$ – 1.5 MeV was delivered to a ^{14}N solid target mounted at 90° with respect to the beam direction and water cooled. A cold trap, made by a tantalum pipe mounted in front of the target was biased at -300 V and kept at liquid nitrogen temperature in order to suppress the secondary electrons and mitigate the carbon buildup on the target, respectively. Typical proton beam intensity was in the range of 200–400 μA .

2.2. γ -ray detectors. – The start of the $^{14}\text{N}(\text{p},\gamma)^{15}\text{O}$ cross-section measurement coincided with the first delivered beam at Bellotti IBF. During this period, a High Purity Germanium (HPGe) detector with 120% relative efficiency⁽²⁾ was installed. The detector was mounted at 55° and at a distance of 45 mm from the target.

In view of a follow-up phase devoted to the angular distribution measurement a table designed to hold an array of three HPGe detectors in place, each of them can be fixed at predefined angles and moved on slits to change their distance from the target. This feature was used to move the detector farther away during target changes and to perform the efficiency calibration (see sect. 3.2).

2.3. Targets. – Extensive development and preparation went into the production of solid nitrogen targets on tantalum backing suitable for the experiment. Two different techniques were employed, reactive sputtering and implantation.

Over the years thin films have been produced to be used as solid targets in nuclear astrophysics experiments via reactive magnetron sputtering of nitride coatings, typically in combination with titanium. This method proved to produce targets with excellent

⁽²⁾ Efficiency expressed here as relative to a standard 3×3 in NaI(Tl) detector, as typically reported by the manufacturers.

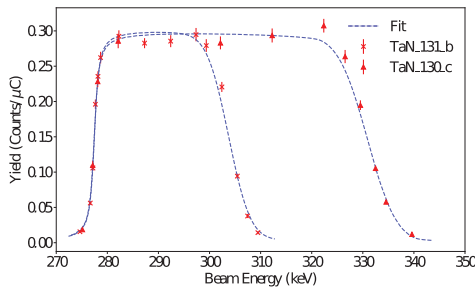
stability against irradiation with high beam power and low concentration of impurities. The higher beam energies achievable at the new facility motivated the development, at the Legnaro National Laboratories, of new targets produced sputtering tantalum nitride (TaN) coatings using enriched (99.95%) ^{14}N gas. This choice was made because the beam-induced background produced by the $^{15}\text{N}(p,\alpha\gamma)^{12}\text{C}$ reaction is problematic especially at the higher energies.

Another type of targets used in the measurement was produced through ^{14}N implantation on Ta backing at the Ion Beam Laboratory of Instituto Técnico Superior, in Lisbon. The main advantage of this type of targets is the isotopic purity of nitrogen that is selected in the implantation process, which makes them naturally devoid of the aforementioned ^{15}N and more suitable for the higher energies. Careful consideration went into the tuning of the implantation parameters (*e.g.*, the ions energy and the total implanted dose), in order to obtain targets with a stable stoichiometry (not oversaturated in ^{14}N inside the tantalum) and a fixed thickness.

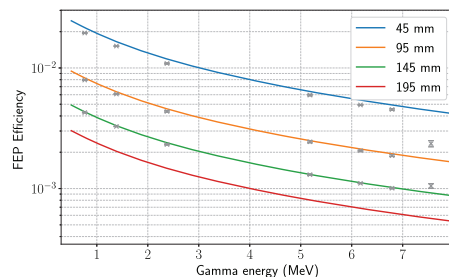
In a preliminary phase a lot of effort went into testing and characterization of the produced targets for both production methods. The samples have been characterized using different ion beam analysis techniques, such as Rutherford Backscattering Spectroscopy (RBS) at their respective production sites in order to obtain stoichiometries and nuclear resonant reaction analysis using the 278 keV resonance of $^{14}\text{N}(p,\gamma)^{15}\text{O}$ at different facilities.

3. – Data analysis

3.1. Targets characterization. – The target thickness and stability of the targets have been tested on site during the irradiations using the 278 keV resonance of $^{14}\text{N}(p,\gamma)^{15}\text{O}$. The measurements have been performed on two different type of TaN-sputtered targets produced with nominal thickness of 2.48×10^{18} atoms/cm² and 1.24×10^{18} atoms/cm², the stoichiometry of the samples was obtained with a 3% uncertainty using the RBS method. Figure 2(a) shows two resonance scans performed during the data taking and fitted in order to obtain the target thickness. The yield profile from the resonance scan has been monitored several times after long irradiations, no evident sign of degradation has been observed.



(a) Resonance scans.



(b) HPGe detector efficiency.

Fig. 2. – On the left, profile scans obtained using the $E_p = 278$ keV resonance on two targets of different thickness. On the right, a plot of the efficiency curves obtained during the measurement (solid lines), together with the experimental yields not corrected for summing effects.

3.2. Detectors efficiency. – The HPGe detectors have been calibrated in efficiency using standard calibrated sources ^{137}Cs and ^{60}Co to fix the low energy region and by $^{14}\text{N}(\text{p},\gamma)^{15}\text{O}$ at 278 keV resonance. All efficiency measurements were performed at different distances in order to investigate the summing-in contribution to the ground-state transition and the summing-out contributions for the transitions to the excited states. The yields Y_i of the γ -rays emitted in the de-excitation through the excited states of ^{15}O , where $i = 6.18, 6.79$ and 5.18 MeV and the one to the ground state $Y_{\text{g.s.}}$, can be expressed, introducing the summing-in and summing-out correction, as:

$$\begin{aligned} (1) \quad Y_i^{\text{pri}} &= R b_i \eta^{\text{FEP}}(E_i^{\text{pri}}) (1 - \eta^{\text{TOT}}(E_i^{\text{sec}})), \\ (2) \quad Y_i^{\text{sec}} &= R b_i \eta^{\text{FEP}}(E_i^{\text{sec}}) (1 - \eta^{\text{TOT}}(E_i^{\text{pri}})), \\ (3) \quad Y_{\text{g.s.}} &= R b_{\text{g.s.}} \eta^{\text{FEP}}(E_{\text{g.s.}}) + R \sum_i b_i \eta^{\text{FEP}}(E_i^{\text{sec}}) \eta^{\text{FEP}}(E_i^{\text{pri}}), \end{aligned}$$

where R is total number of reaction per unit charge and b_i is the branching ratio of the specific transition and $\eta^{\text{FEP},\text{TOT}}$ represent the full-energy peak and total efficiency of the detector. These two functions can be expressed using a standard parametrization and obtained by performing a fit of the experimentally observed yields measured at different distances from the target, as shown in [4]. The resulting efficiency curves as a function of γ -ray energy obtained with this approach are reported in fig. 2(b).

4. – Preliminary results and discussion

During the measurement, cross-section data have been collected with one HPGe detector placed at 55° in the energy range $E_p = 0.25\text{--}1.5$ MeV, for a total of 38 C of charge accumulated on 4 different targets.

Preliminary cross-section results (*i.e.*, the experimental yield, corrected for the target thickness and summing effects) are presented for the 6.79 MeV and 5.24 MeV secondary transitions and for the ground state in fig. 3. Moreover, most of the other weaker transitions, many of them not observed by previous authors (Schröder *et al.* [5]) are identifiable in the spectra and will be included in a comprehensive analysis of the data set in progress.

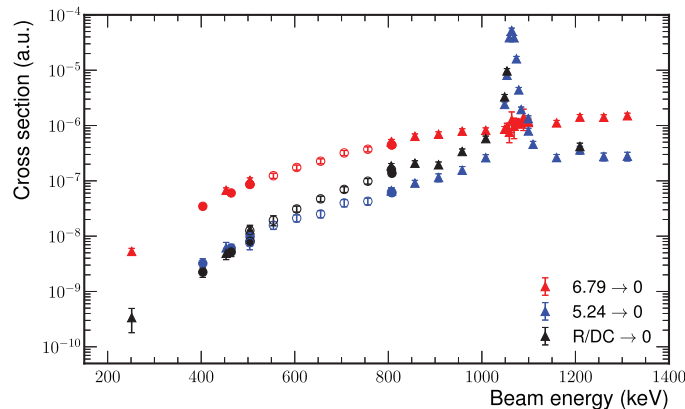


Fig. 3. – Preliminary cross-sections data for ground state, 6.79 MeV and 5.24 MeV secondary transitions, obtained with one HPGe detector placed at 55° .

In a close future phase of the experiment the angular distributions of the most important transitions of the reaction will be measured, most notably going below 600 keV where no literature data are available.

Additionally, these preliminary results showcase the strength of measuring this reaction taking advantage from the high current and excellent long-term stability of the beam produced by the 3.5 MV accelerator of the Bellotti IBF paired with the extremely low background conditions present in its underground location.

* * *

The author acknowledge Donatello Ciccotti and Massimo Orsini as part of the Accelerator Service of LNGS for their technical support.

REFERENCES

- [1] ADELBERGER E. G. *et al.*, *Rev. Mod. Phys.*, **83** (2011) 195.
- [2] BAHCALL J. N. *et al.*, *Astrophys. J.*, **621** (2005) L85.
- [3] APPEL S. *et al.*, *Phys. Rev. Lett.*, **129** (2022) 252701.
- [4] IMBRIANI G. *et al.*, *Eur. Phys. J. A*, **25** (2005) 455.
- [5] SCHROÖDER U. *et al.*, *Nucl. Phys. A*, **467** (1987) 240.
- [6] RUNKLE R. C. *et al.*, *Phys. Rev. Lett.*, **94** (2005) 082503.
- [7] LI Q. *et al.*, *Phys. Rev. C*, **93** (2016) 055806.
- [8] FRENTZ B. *et al.*, *Phys. Rev. C*, **106** (2022) 065803.
- [9] WAGNER L. *et al.*, *Phys. Rev. C*, **97** (2018) 015801.
- [10] MARTA M. *et al.*, *Phys. Rev. C*, **78** (2008) 022802.
- [11] DAIGLE S. *et al.*, *Phys. Rev. C*, **94** (2016) 025803.
- [12] FRENTZ B. *et al.*, *Phys. Rev. C*, **103** (2021) 045802.
- [13] GYÜRKY G. *et al.*, *Phys. Rev. C*, **105** (2022) L022801.
- [14] JUNKER M. *et al.*, *Front. Phys.*, **11** (2023) 1291113.